THE ASTROPHYSICAL JOURNAL, 460:L119–L122, 1996 April 1

VARIATIONS OF THE 8.6 AND 11.3 μm EMISSION BANDS WITHIN NGC 1333: EVIDENCE FOR POLYCYCLIC AROMATIC HYDROCARBON CATIONS

C. JOBLIN,[1,2] A. G. G. M. TIELENS,[1] T. R. GEBALLE,[3] AND D. H. WOODEN[1]
Received 1995 December 6; accepted 1996 January 19

ABSTRACT

We have obtained 8–13 μm spectra of three positions in the IR reflection nebula associated with SVS 3 in NGC 1333. These observations reveal systematic variations in the relative intensities of the IR emission features at 8.6 μm and 11.3 μm. In particular, the [8.6]/[11.3] ratio is highest at the position of the exciting star and decreases with increasing angular distance from the star. We attribute these variations to changes in the relative populations of ionized and neutral polycyclic aromatic hydrocarbons (PAHs), driven by the strong far-ultraviolet radiation field near the star. From experiments and quantum chemical theoretical studies, the intrinsic strength of these two bands is known to vary with the charge state of the emitting PAH. We have developed a simple model for the relative intensity of the 8.6 and 11.3 μm bands taking the charge state of the carrier into account. This model is in good agreement with the data. We point out several observational and experimental tests of this model.

Subject headings: dust, extinction — infrared: ISM: lines and bands — ISM: individual (NGC 1333) — reflection nebulae

1. INTRODUCTION

The carriers of the so-called unidentified IR (UIR) bands, whose main components are located at 3.3, 6.2, 7.7, 8.6, and 11.3 μm, are generally thought to be carbonaceous and dominated by aromatic bonds. Among the various candidates are polycyclic aromatic hydrocarbon molecules and their ions (PAHs; Léger & Puget 1984; Allamandola, Tielens, & Barker 1985), hydrogenated amorphous carbons (HAC; Borghesi, Bussoletti, & Colangeli 1987), quenched carbonaceous components (QCC; Sakata et al. 1984, 1987) and coal grains (Papoular et al. 1989).

The UIR bands are found in reflection nebulae, planetary nebulae, and H II regions (see, e.g., Cohen et al. 1986, 1989, and references therein), and are observed in many galaxies. In addition, they are present in the diffuse interstellar medium as shown by the AROME measurements at 3.3 and 6.2 μm (Giard et al. 1988; Ristorcelli et al. 1994). Therefore, their carriers are an important and widespread component of the interstellar medium.

Of the various candidates that have been proposed as carriers of the bands, none has yet provided a fully satisfactory match to all of the observed characteristics of the emission features. Although the properties of the candidates should be better explored, more astronomical observations also are needed to provide additional spectral and spatial details, relate the behaviors of the various bands to one another, and stimulate meaningful laboratory and theoretical work. In particular, measurements of the variations of the UIR bands in changing physical and chemical conditions, caused for example by different radiation fields, densities, or elemental abundances, often give new clues on the chemical structure of the band carriers. Studies of (large) samples of astronomical objects (e.g., Jourdain de Muizon, d'Hendecourt, & Geballe 1990a; Zavagno, Cox, & Baluteau 1992) provide observations covering a range of physical conditions. An alternative approach, used for instance by Geballe et al. (1989), Roche, Aitken, & Smith (1994), Joblin et al. (1996), and in this paper, is making spatial studies within individual extended objects. Due to geometric dilution and dust extinction, some of the physical parameters (e.g., UV intensity) vary in predictable ways over these objects, and changes in UIR bands may be linked to them.

A recent study of the reflection nebula in NGC 1333 excited by the star SVS 3 has shown that within it there are large changes in the relative intensities of the 3.3 μm band and its main satellite band at 3.4 μm (Joblin et al. 1996). These variations were found to correlate with those of the UV field intensity and were successfully modeled by photodissociation of aliphatic subgroups attached to PAH molecules. In this paper, a similar study of NGC 1333 SVS 3 is made using the UIR bands at 8.6 and 11.3 μm.

2. OBSERVATIONS AND DATA REDUCTION

Spectra of NGC 1333 were obtained at the 3.8 m United Kingdom Infrared Telescope (UKIRT) by its 32 channel grating spectrograph, CGS3, as part of the UKIRT Service program. The observations, made on 1995 January 14 and 1995 August 20, employed CGS3's 5″ diameter aperture and its low resolution 10 μm grating, set to cover 7.4–13.2 μm at $R \sim 60$. Three positions were observed: the exciting star (SVS 3), 5″.5 south, and 11″.0 south. The UKIRT observations were prompted by the 1994 November observations with HIFOGS (Witteborn et al. 1995) at the NASA 1.5 m Mount Lemmon Observatory, which, although of low signal-to-noise ratio, provided the first evidence for a significant variation in the relative strengths of the mid-IR unidentified bands within the nebula.

Standard chopping (5 Hz) and nodding techniques were used, with the reference beams 30″ east and west of the observed position in the nebula. The spectra were sampled

[1] NASA Ames Research Center, MS: 245-6, Moffett Field CA 94035; tielens@dusty.arc.nasa.gov, wooden@ssa1.arc.nasa.gov.

[2] Present address: Centre d'Etude Spatiale des Rayonnements, UPR-CNRS 8002, 9 Avenue du Colonel Roche, BP 4346, 31029 Toulouse Cedex, France; joblin@cesr.cnes.fr.

[3] Joint Astronomy Centre, 660 N. A'ohoku Pl., Hilo HI 96720; tom@jach.hawaii.edu.

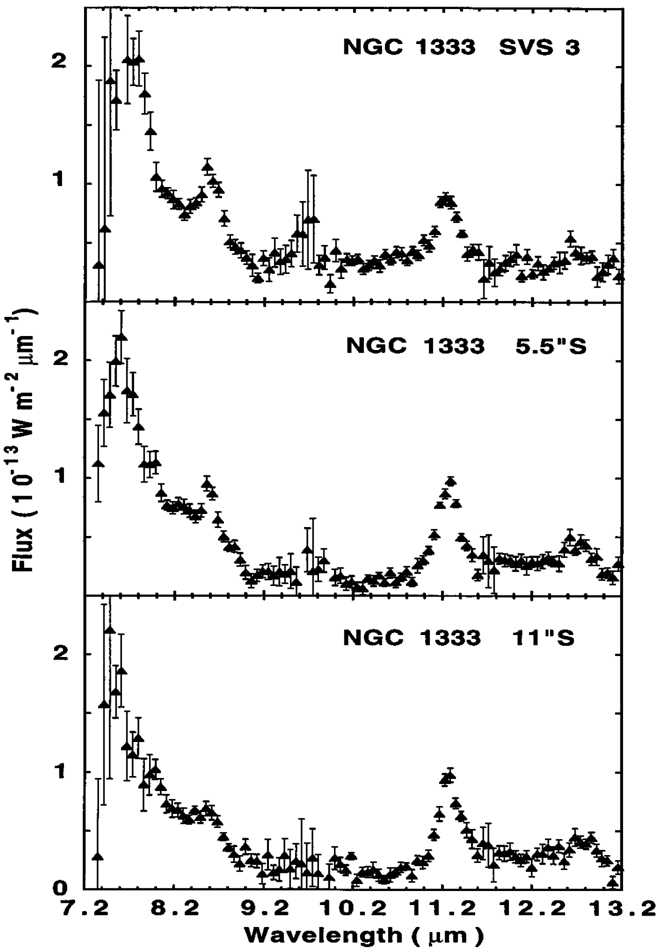

FIG. 1.—Spectra of NGC 1333 at three locations; offsets are relative to the exciting star SVS 3. Error bars are $\pm 1\ \sigma$.

every $\frac{1}{3}$ resolution element. BS 1708 was employed as the standard star and assumed to have N magnitude -1.94 and blackbody temperature 5200 K. Wavelength calibration was achieved by observing the 2 μm lines of a Krypton lamp in orders 4–6.

Flux- and wavelength-calibrated spectra derived from the 1995 August 20 measurements are shown in Figure 1. Integration times were 18 minutes at SVS 3 and 11″ south, and 24 minutes at the 5″.5 south position. The large error bars at the short wavelength edge of the spectra are due to the atmospheric and filter cut-offs. Those at 9.7 μm are due to the telluric ozone absorption band; those near 11.7 μm are due to a noisy detector.

3. RESULTS

The spectra of NGC 1333 in Figure 1 clearly exhibit the well-known UIR emission bands at 7.7 μm, 8.6 μm, and 11.3 μm. The 8.6 μm feature is on the wing of the stronger 7.7 μm feature. In both the January and August CGS3 spectra, the 8.6 μm feature at SVS 3 appears more prominently than in the somewhat lower resolution and less finely sampled spectrum of Roche et al. (1994). The asymmetric profile of the 11.3 μm feature is similar to that seen by Roche et al. (1994) and in other objects by Witteborn et al. (1989). A weaker band at 12.7 μm, also known to be part of the family of UIR emission bands, is detected at all three locations, but most easily off the star. This band is superposed on a plateau, extending from the 11.3 μm feature to 13 μm. A weak plateau at about 10 μm (from ~9.2 to ~11.2 μm) may be present at the star position and may be due to emission by silicates.

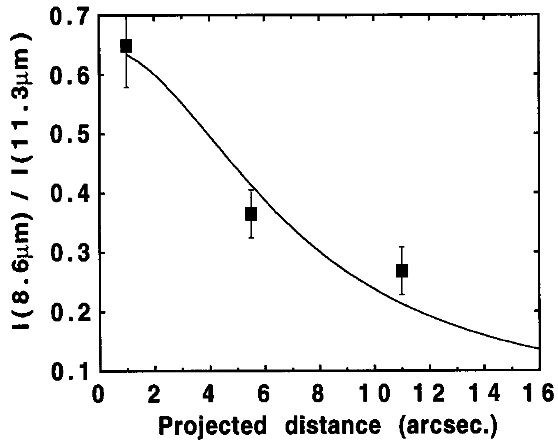

FIG. 2.—Model fit of the ratio of the 8.6 to 11.3 μm band intensities in NGC 1333 as a function of angular distance from SVS 3, including emission from both neutral PAHs and PAH cations. The observed values of the ratio, derived from Fig. 1, are also shown.

The most significant finding from these observations is the different spatial behavior of the intensity of the 8.6 μm feature from that of the 11.3 μm feature. The intensity of the 8.6 μm feature is high on the exciting star and markedly decreases with angular distance from the star. In contrast, the intensity of the 11.3 μm band intensity increases with increasing distance from the star, as does the 3.3 μm band intensity (Joblin et al. 1996).

The spatial variations of the 7.7 μm band are difficult to assess, due to the poor atmospheric transmission near that wavelength. Only the long wavelength wing of the band is easily observable from the ground, precluding accurate quantification of the feature's integrated intensity.

4. DISCUSSION

4.1. *Variation of the Relative UIR Band Intensities in Other Objects*

The data presented here demonstrate that there is a large variation of the ratio of 8.6 to 11.3 μm band intensities with distance from the exciting star of NGC 1333, SVS 3 (see Fig. 2). Spatial variations of relative intensities of several UIR bands have been reported previously. Sloan, Grasdalen, & LeVan (1993) observed that the 7.7 μm feature drops more quickly with distance from the central star of the Red Rectangle, HD 44179, than the 8.6 and 11.3 μm features. They suggested that this is due to the hydrogen coverage of the emitting material increasing with distance from the central star. Bregman et al. (1993a) showed that the similar north-south extent of the images of the same object at 3.3 and 11.3 μm implies that the ratio of small-to-large PAHs does not change substantially with distance from HD 44179. In the Orion Bar, Roche, Aitken, & Smith (1989) observed that the underlying continuum (11–13 μm) falls off more slowly than the bands at 11.3 and 12.7 μm. Bregman et al. (1989) showed that the 3.3 and 11.3 μm features are well correlated spatially while the 7.7 μm band has a different distribution. They explained these variations in terms of increasing dehydrogenation closer to the H II region.

In several nebulae including NGC 1333, the intensity ratio of the 3.4 to 3.3 μm bands has been observed to increase with distance from the exciting star (Geballe et al. 1989; Joblin et al. 1996). Joblin et al. explained the behavior of the 3 μm bands in terms of increased photodissociation near the star of methyl sidegroups attached to the PAHs which are thought to be responsible for the 3.4 μm emission (Jourdain de Muizon, d'Hendecourt & Geballe 1990b). The variations of the 8.6 and 11.3 μm bands observed in NGC 1333 also may be tracers of related photochemical behavior of their carriers.

4.2. *PAH Cations and the* [8.6]/[11.3] *Ratio*

Spatial variations of the 8.6 and 11.3 μm bands relative to each other may seem surprising if these bands are attributed to the CH bending modes (in-plane and out-of-plane, respectively) of neutral PAH molecules. However, quantum chemistry calculations (DeFrees et al. 1993; Pauzat, Talbi, & Ellinger 1994; Langhoff 1995) and laboratory experiments (see, for instance, Szczepanski & Vala 1993a, 1993b; Hudgins & Allamandola 1995a, 1995b) have shown that the IR band intensities of PAHs are strongly dependent on ionization state. The intensities of the CC stretching and CH in-plane bending modes, which fall in the 6–9 μm range, are generally an order of magnitude stronger in PAH cations (singly ionized PAHs) than PAH neutrals. The effects of ionization state on the CH out-of-plane bending (11–14 μm) mode intensities are quite different, although not so clearly defined. Laboratory studies indicate that their intensities decrease upon ionization, although an average factor of 2 is reported by Szczepanski & Vala (1993a, 1993b) whereas a factor of 5–20 is reported by Hudgins & Allamandola (1995a). Quantum chemistry calculations, on the other hand, do not predict significant changes.

Thus, the observed variations in the [8.6]/[11.3] ratio in NGC 1333 can be linked to variations in the charge state of the emitting PAHs. In this interpretation, the PAHs near SVS 3 are ionized, producing a high [8.6]/[11.3] ratio. Farther from the star, the FUV field is reduced by geometric dilution, the PAHs are more neutral, and the [8.6]/[11.3] ratio is lower.

4.3. *Modeling the Emission from PAH Neutrals and Cations*

The ionized fraction of PAHs is determined by the competition between the absorption of the UV photons which lead to ionization of the molecule, and the neutralization of the positively charged ion by collision with electrons (Verstraete et al. 1990; Bakes & Tielens 1994). For a distribution of molecules, the balance may be quite complicated, as the sizes and shapes of the molecules are important (Salama et al. 1996). In this letter, we consider a single size of $N_c = 100$ carbon atoms. The ionization balance is given by

$$n_n R_{\rm ion} = n_p \alpha n_e, \qquad (1)$$

where n_n and n_p are the density of neutral PAHs and cations respectively, $R_{\rm ion}$ the ionization rate, α the recombination rate with electrons, and n_e the electronic density.

To estimate $R_{\rm ion}$, we use a mean value of the ionization cross-section, $\langle\sigma_{\rm ion}\rangle = 5 \times 10^{-18}$ cm^2 per carbon atom deduced from laboratory measurements on coronene (Verstraete et al. 1990), and express the integral of the UV field in terms of the Habing field, G_o (Habing 1968). In NGC 1333, we have estimated (Joblin et al. 1996) that $G_o = 4.8 \times 10^5$ at 1″ from the star ($G_o = 1$ corresponds to 10^8 photons cm^{-2} s^{-1} in the diffuse medium). The decrease of the UV field with distance from the star is assumed to be due solely to the geometrical dilution, which seems reasonable for this object (see Joblin et al. 1996).

The emission at 8.6 and 11.3 μm results from the contribution of neutrals and cations. We can easily derive

$$\frac{I(8.6\ \mu\text{m})}{I(11.3\ \mu\text{m})} = \frac{I_n(8.6\ \mu\text{m})}{I_n(11.3\ \mu\text{m})} \times \left\{\left[1 + \frac{n_p}{n_n}\frac{I_p(8.6\ \mu\text{m})}{I_n(8.6\ \mu\text{m})}\right] \Big/ \left[1 + \frac{n_p}{n_n}\frac{I_p(11.3\ \mu\text{m})}{I_n(11.3\ \mu\text{m})}\right]\right\}, \qquad (2)$$

where I_n and I_p are emission intensities of neutrals and cations respectively, and n_p/n_n is the fraction of ionized to neutral PAHs given by equation (1). We assume all carbon to be ionized and adopt $n_e = 3 \times 10^{-4}\ n_{\rm H}$ with $n_{\rm H} = 5 \times 10^4$ cm^{-3} (Joblin et al. 1996), $N_c = 100$ and I_p (8.6 μm)/I_n (8.6 μm) = 10 (see above). In the thermal approximation (Léger et al. 1989), $I(\lambda_i) = B_{\lambda_i}(T_{em})\,A(\lambda_i)$ with $B_{\lambda_i}(T_{em})$ the Planck function at the temperature T_{em} and $A(\lambda_i)$ the intrinsic integrated strength of the band centered at λ_i. The value of the average emission temperature (defined in Léger et al.) is 554 K for a 100 C-atom molecule after absorption of a 10 eV photon. Using gas-phase measurements on neutral PAHs (see Table 7 in Joblin et al. 1994), we then deduce that I_n (8.6 μm)/I_n(11.3 μm) = 1/26.

Electron recombination coefficients have been estimated using classical electrostatics to be about 3×10^{-5} cm^3 s^{-1} for a 100 C-atom PAH at 100 K (Verstraete et al. 1990; Bakes & Tielens 1994). However, the experimentally measured values of 1×10^{-6} and 3×10^{-7} for ionized benzene and naphthalene at 300 K (Abouelaziz et al. 1993) are much less than the classical estimates for these small PAHs. While it is likely that the electron recombination coefficient for large PAHs approaches the classical estimates, we treat α as a free parameter and derive the best-fit value. Similarly, as discussed in § 4.2, the value for I_p(11.3 μm)/I_n(11.3 μm) is uncertain and we also treat it as a free parameter. The fit of the data points in Figure 2 using equation (2) leads to $\alpha = 1.9 \times 10^{-5}$ cm^3 s^{-1} and I_p(11.3 μm)/I_n(11.3 μm) = 0.6 with a correlation coefficient $r = 0.96$. These values are reasonable and indicate that the ratio I(8.6 μm)/I(11.3 μm) is well represented by equation (2). Therefore, the two features at 8.6 and 11.3 μm may be carried by a mixture of PAH neutrals and cations, with the 8.6 μm band effectively being the tracer of the ionized population. Evaluation of equation (1) indicates that the ionization fraction is 100% at the star position (Fig. 1 [*top*]) and about 40% at 11″ south (Fig. 1 [*bottom*]). These results should be investigated further, in particular when more observations and more molecular data (values of α and I_p(11.3 μm) for large molecules) are available.

5. CONCLUSION

In this Letter it has been shown that predicted spatial changes in the ratio of ionized-to-neutral PAH molecules can account in a simple way for the variation of the 8.6 to 11.3 μm band intensity ratio in NGC 1333. There is firm experimental and quantum chemical evidence that the charge state of PAHs affects the relative intensities of these bands. In addition, it is expected that PAHs in nebulae are charged and that their ionization state varies with FUV intensity. The charge state of interstellar PAHs is expected to vary considerably in the interstellar medium (ISM) depending on the local physical conditions (Salama et al. 1996). We expect, therefore, that the IR emission spectrum of the ISM will show similar variations to those observed within NGC 1333 here. The infrared satellite *ISO* is well suited to search for them. It remains to be seen whether there is a straightforward explanation for the observed variations in relative intensities of the 8.6 and 11.3 μm features if these features arise from carbonaceous grains.

However, until more data are available, our interpretation must be regarded as tentative and qualitative. In particular, the electronic recombination coefficient and the intensity of the 11.3 μm band for large ionized PAHs must be better characterized experimentally and theoretically. Observations of more nebulae at higher spatial resolution also are needed. Bregman et al. (1993b) obtained high resolution maps of NGC 1333 at 3.3 and 11.3 μm, and showed that the two emission features come from spatially distinct regions. Similar studies of the 8.6 μm emission should be made, especially if this feature is a tracer of ionized PAHs. The ionization of PAHs should lead not only to an increase of the 8.6 μm feature, but also to an increase of the 6.2 and 7.7 μm features. Testing this prediction will be an important task for the IR camera on *ISO*.

We wish to acknowledge the UKIRT Service program and thank the staff of UKIRT for its support of this research.

REFERENCES

Abouelaziz, H., Gomet, J. C., Pasquerault, D., Rowe, B. R., & Mitchell, J. B. A. 1993, J. Chem. Phys., 99, 237
Allamandola, L. J., Tielens, A. G. G. M., & Barker, J. R. 1985, ApJ, 290, L25
Bakes, E. L. O., & Tielens, A. G. G. M. 1994, ApJ, 427, 822
Borghesi, A., Bussoletti, E., & Colangeli, L. 1987, ApJ, 314, 422
Bregman, J. D., Allamandola, L. J., Tielens, A. G. G. M., Geballe, T. R., & Witteborn, F. C. 1989, ApJ, 344, 791
Bregman, J. D., Rank, D., Sandford, S. A., & Temi, P. 1993b, ApJ, 410, 668
Bregman, J. D., Rank, D., Temi, P., Hudgins, D., & Kay, L. 1993a, ApJ, 411, 794
Cohen, M., Allamandola, L., Tielens, A. G. G. M., Bregman, J., Simpson, J. P., Witteborn, F. C., Wooden, D., & Rank, D. 1986, ApJ, 302, 737
Cohen, M., Tielens, A. G. G. M., Bregman, J., Witteborn, F. C., Rank, D. M., Allamandola, L. J., Wooden, D., & de Muizon, M. 1989, ApJ, 341, 246
DeFrees, D. J., Miller, M. D., Talbi, D., Pauzat, F., & Ellinger, Y. 1993, ApJ, 408, 530
Geballe, T. R., Tielens, A. G. G. M., Allamandola, L. J., Moorhouse, A., & Brand, P. W. J. L. 1989, ApJ, 341, 278
Giard, M., Pajot, F., Lamarre, J. M., Serra, G., Caux, E., Gispert, R., Léger, A., & Rouan, D. 1988, A&A, 201, L1
Habing, H. J. 1968, Bull. Astron. Inst. Netherlands, 19, 421
Hudgins, D. M., & Allamandola, L. J. 1995a, J. Phys. Chem., 99, 3033
———. 1995b, J. Phys. Chem., 99, 8978
Joblin, C., d'Hendecourt, L., Léger, A., & Défourneau, D. 1994, A&A, 281, 923
Joblin, C., Tielens, A. G. G. M., Allamandola, L., & Geballe, T. R. 1996, ApJ, 458, 610
Jourdain de Muizon, M., d'Hendecourt, L. B., & Geballe, T. R., 1990a, A&A, 227, 526
Jourdain de Muizon, M., d'Hendecourt, L. B., & Geballe, T. R., 1990b, A&A, 235, 367
Langhoff, S. R. 1995, preprint
Léger, A., d'Hendecourt, L., & Défourneau, D. 1989, A&A, 216, 148
Léger, A., & Puget, J. L. 1984, A&A, 137, L5
Papoular, R., Conard, J., Guiliano, M., Kister, J., & Mille, G. 1989, A&A, 217, 204
Pauzat, F., Talbi, D., & Ellinger, Y. 1994, in Molecules and Grains in Space, ed. I. Nenner, (New York: AIP), 635
Ristorcelli, I., Giard, M., Mény, C., Serra, G., Lamarre, J. M., Le Naour, C., Léotin, J., & Pajot, F. 1994, A&A, 286, L23
Roche, P. F., Aitken, D. K., & Smith, C. H. 1989, MNRAS, 236, 485
———. 1994, MNRAS, 269, 649
Sakata, A., Wada, S., Onaka, T., & Tokunaga, A. T. 1987, ApJ, 320, L63
Sakata, A., Wada, S., Tanabe, T., & Onaka T. 1984, ApJ, 287, L51
Salama, F., Bakes, E. L. O., Allamandola, L. J., & Tielens, A. G. G. M. 1996, ApJ, 458, 621
Sloan, G. C., Grasdalen, G. L., & LeVan, P. D. 1993, ApJ, 409, 412
Szczepanski, J., & Vala, M. 1993a, Nature, 363, 699
———. 1993b, ApJ, 414, 646
Verstraete, L., Léger, A., d'Hendecourt, L., Dutuit, O., & Défourneau, D. 1990, A&A, 237, 436
Witteborn, F. C., Cohen, M., Bregman, J. D., Heere, K. R., Greene, T. P., & Wooden, D. H. 1995, in ASP Conf. Ser. 73, Proceedings of the Airborne Astronomy Symposium on the Galactic Ecosystem, ed. M. Haas, E. F. Erickson, & J. Davidson (San Francisco: ASP), 573
Witteborn, F. C., Sandford, S. A., Bregman, J. D., Allamandola, L. J., Cohen, M., Wooden, D. H., & Graps, A. L. 1989, ApJ, 341, 270
Zavagno, A., Cox, P., & Baluteau, J. P. 1992, A&A, 259, 241